

VLT polarimetry observations of the middle-aged pulsar PSR B0656+14[★] (Research Note)

R. P. Mignani^{1,2}, P. Moran³, A. Shearer³, V. Testa⁴, A. Słowikowska², B. Rudak⁵, K. Krzeszowski², and G. Kanbach⁶

¹ INAF–Istituto di Astrofisica Spaziale e Fisica Cosmica Milano, via E. Bassini 15, 20133 Milano, Italy
e-mail: mignani@iasf-milano.inaf.it

² Janusz Gil Institute of Astronomy, University of Zielona Góra, Lubuska 2, 65-265 Zielona Góra, Poland

³ Centre for Astronomy, School of Physics, National University of Ireland Galway, University Road, Galway, Ireland

⁴ INAF–Osservatorio Astronomico di Roma, via Frascati 33, 00040 Monteporzio, Italy

⁵ Nicolaus Copernicus Astronomical Center, ul. Rjabiańska 8, 87100 Toruń, Poland

⁶ Max-Planck Institut für Extraterrestrische Physik, Giessenbachstrasse 1, 85741 Garching bei München, Germany

Received 29 July 2015 / Accepted 5 October 2015

ABSTRACT

Context. Optical polarisation measurements are key tests for different models of the pulsar magnetosphere. Furthermore, comparing the relative orientation of the phase-averaged linear polarisation direction and the pulsar proper motion vector may unveil a peculiar alignment, clearly seen in the Crab pulsar.

Aims. Our goal is to obtain the first measurement of the phase-averaged optical linear polarisation of the fifth brightest optical pulsar, PSR B0656+14, which also has a precisely measured proper motion, and to verify a possible alignment between the polarisation direction and the proper motion vector.

Methods. We carried out observations with the Very Large Telescope (VLT) to measure the phase-averaged optical polarisation degree (PD) and position angle (PA) of PSR B0656+14.

Results. We measured a PD of $11.9\% \pm 5.5\%$ and a PA of $125.8^\circ \pm 13.2^\circ$, measured east of north. Albeit of marginal significance, this is the first measurement of the phase-averaged optical PD for this pulsar. Moreover, we found that the PA of the phase-averaged polarisation vector is close to that of the pulsar proper motion ($93.12^\circ \pm 0.38^\circ$).

Conclusions. Deeper observations are needed to confirm our polarisation measurement of PSR B0656+14, whereas polarisation measurements for more pulsars will better assess possible correlations of the polarisation degree with the pulsar parameters.

Key words. pulsars: individual: PSR B0656+14 – pulsars: general – polarization

1. Introduction

Polarisation measurements of pulsars offer unique insights into their highly-magnetised relativistic environments and are a primary test for neutron star magnetosphere models and radiation emission mechanisms. Besides the radio band, optical observations are best suited to these goals. Indeed, significant polarisation is expected when the optical emission is produced by synchrotron radiation in the neutron star magnetosphere. Owing to their faintness, linear optical polarisation measurements only exist for a handful of pulsars, whereas the circular polarisation was only measured for the Crab pulsar (Wiktorowicz et al. 2015). The young (~ 960 year old) and bright ($V \sim 16.5$) Crab pulsar (PSR B0531+21) is the only one for which precise measurements have been repeatedly obtained, both phase-resolved (e.g., Słowikowska et al. 2009) and phase-averaged (e.g., Moran et al. 2013). Interestingly, the phase-averaged optical polarisation position angle is similar to that of the pulsar proper motion direction and close to that of the axis of symmetry of the X-ray arcs and jets of the pulsar-wind nebula (PWN) observed by *Chandra* (e.g. Hester 2008), which is also assumed

to be the pulsar spin axis. This kind of approximate alignment, might trace the connection between the pulsar magnetospheric emission, its dynamical interaction with the PWN, and the neutron star formation, with the kick and spin axis directions determined at birth. Evidence of a similar alignment has been found from optical polarisation measurements of the Vela pulsar (PSR B0833–45; $V \sim 23.6$) by Mignani et al. (2007) and Moran et al. (2014), whereas for both PSR B0540–69 ($V = 22.5$) and PSR B1509–58 ($R = 25.7$) the lack of a measured proper motion makes it impossible to check the alignment with the polarisation direction (Mignani et al. 2010; Lundqvist et al. 2011; Wagner & Seifert 2000). The next best target is PSR B0656+14, the brightest pulsar detected in the optical after Vela (Mignani 2011). PSR B0656+14 ($V \sim 25$) is a middle-aged ($\sim 10^5$ years) optical pulsar (Shearer et al. 1997; Kern et al. 2003; Kargaltsev & Pavlov 2007) with strong magnetospheric optical emission (e.g. Zharikov et al. 2007). It is not embedded in a bright and variable optical PWN and its supernova remnant (SNR) has already faded away in the interstellar medium (ISM), which minimises the local background polarisation. Moreover, at a distance of 0.28 ± 0.03 kpc (Verbiest et al. 2012), PSR B0656+14 is affected by a relatively low foreground polarisation. Last but not least, it has an extremely accurate radio proper motion ($\mu = 44.13 \pm 0.63$ mas yr⁻¹; Brisken et al. 2003), which makes

[★] Based on observations collected at ESO, Paranal, under Programme 090.D-0106(A).

it possible to search for a possible alignment with the phase-averaged polarisation direction.

Here, we report on the first phase-averaged linear polarisation observations of PSR B0656+14, performed with the Very Large Telescope (VLT).

2. Observations and data analysis

We observed PSR B0656+14 between January and February 2014 with the second version of the Focal Reducer and low dispersion Spectrograph (FORS; Appenzeller et al. 1998) at the VLT Antu telescope. FORS2 is equipped with a mosaic of two $4k \times 2k$ MIT CCDs aligned along the Y axis, optimised for wavelengths longer than 6000 \AA . Observations were performed in imaging polarimetry mode (IPOL), with standard low gain, normal readout (200 Kpix/s), standard-resolution mode ($0''.25/\text{pixel}$), and the high efficiency V-band filter (v_{HIGH} ; $\lambda = 555.0 \text{ nm}$, $\Delta\lambda = 61.6 \text{ nm}$). For all the observations, the target was at the nominal aim position on the upper CCD chip (CHIP1) to avoid the effects of instrumental polarisation at the CCD edges. The FORS2 polarisation optics consist of a Wollaston prism as a beam splitting analyser and two super-achromatic phase retarder 3×3 plate mosaics installed on rotatable mountings that can be moved in and out of the light path. Images are obtained by taking two frames displaced by $22''$ in the direction perpendicular to the Multi-Object Spectrograph (MOS) slitlets. We used the four standard IPOL half-wave retarder plate angles of 0° , 22.5° , 45° , and 67.5° , corresponding to the retarder plate orientation with respect to the Wollaston prism and usually set with an accuracy $\lesssim 0.1^\circ$ (Boffin 2014). Both the axis of the detector optics and the zero point of the half wave retarder plate angle are set such that the polarisation position angle is measured eastward from north.

To avoid introducing spurious effects due to the variable sky polarisation background across different nights, each of the nine observation blocks (OBs) incorporated exposures for all the four retarder plate angles (715 s each). Observations were executed in dark time, with a seeing of $0''.6$ – $1''.3$, airmass below 1.4, and in clear sky conditions. Short exposures (< 3 s) of both polarised and unpolarised standard stars were also acquired for calibration. Twilight flat-field images with no retarder plate along the light path were also acquired on the same nights as the science images. For both the pulsar and standard stars, single-exposure raw images were bias-subtracted and flat-fielded using standard routines in IRAF¹. We computed the FORS2 astrometry using stars from the Guide Star Catalogue 2 (GSC-2; Lasker et al. 2008) as a reference. After accounting for all uncertainties (star centroids, GSC-2 absolute coordinate accuracy) our astrometric solution turned out to be $\lesssim 0''.1$ rms. PSR B0656+14 (Fig. 1) is detected at the position expected by extrapolating its proper motion (Brisken et al. 2013) to the epoch of our observations, where the uncertainty in the proper motion extrapolation is well below that in our astrometry calibration.

In order to increase the signal-to-noise, we co-added all the nine reduced science images of PSR B0656+14 taken with the same retarder plate angle. For each angle, we aligned the single images using the IRAF tasks `ccdmap` and `ccdtrans`, with an average accuracy of a few hundreds of a pixel. We applied the image co-addition with the routine `combine` and filtered cosmic

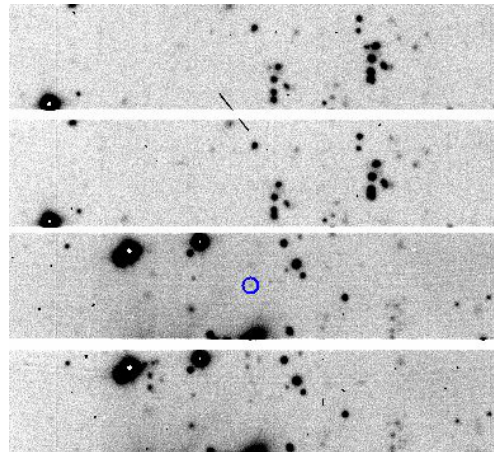


Fig. 1. Image of the PSR B0656+14 field (715 s) taken with the 0° retarder plate angle. The pair of images ($22''$ height) correspond to the extraordinary and ordinary beams. The pulsar counterpart is circled.

ray hits using the *pclip* algorithm. Then, we measured the pulsar flux in each of the four co-added images through PSF photometry with the package *daophot* (Stetson 1994) implemented in IRAF. In particular, we fitted the model PSF to the pulsar intensity profile within an area of 10 pixel radius ($2''.5$), estimated from the growth curves of reference stars. We measured the sky background in an annulus of inner radius of 10.5 pixels and width of 10 pixels ($2''.6$ and $2''.5$), respectively, centred on the pulsar position. We carefully tailored this annulus both to avoid the wings of the pulsar intensity profile and accurately sample the sky background without being sensitive to strong fluctuations and gradients in the background level. We corrected the pulsar flux for the atmospheric extinction using, for each image, the average airmass value and extinction coefficients in the v_{HIGH} filter². We followed Fossati et al. (2007) to compute the errors in PD and PA. From the observations of the polarised standards, the absolute calibration of our polarimetry is accurate to $\sim 0.1\%$ in PD and to $\lesssim 0.5^\circ$ in PA, whereas from the observations of the unpolarised standards we found no evidence of significant instrumental polarisation at the CHIP1 aim position and no systematic deviations in the zero point of the retarder half wave plate angle. For the photometry parameters defined above, we measured a PD = $11.9\% \pm 5.5\%$ and a PA = $125.8^\circ \pm 13.2^\circ$, where the associated errors account both for statistical errors and calibration uncertainties.

3. Discussion

Although of marginal significance ($\sim 2.2\sigma$), but still comparable to those obtained for other pulsars (Mignani et al. 2007; Lundqvist et al. 2011), ours is the first and only measurement of the phase-averaged optical polarisation degree of PSR B0656+14 obtained so far. Indeed, no value of the phase-averaged polarisation was reported from the phase-resolved polarimetry observations of Kern et al. (2003). Their measurements show that the bridge between the two peaks of the optical light curve seems to be strongly polarised (PD $\approx 100\%$), whereas the peaks seem to be unpolarised (PD $\approx 0\%$). However, the large errors ($\pm 40\%$ at 1σ) attached to the phase-resolved polarisation values in each phase bin strongly affect the significance of their result. Nonetheless, this large variation of the PD would suggest

¹ IRAF is distributed by the National Optical Astronomy Observatories, which are operated by the Association of Universities for Research in Astronomy, Inc., under cooperative agreement with the National Science Foundation.

² www.eso.org/qc

Table 1. Summary of the phase-average linear polarisation measurements for pulsars detected in the optical.

Pulsar	τ (10^3 yr)	P_s (s)	\dot{P}_s (10^{-13} s s $^{-1}$)	\dot{E} (10^{38} erg cm $^{-2}$ s $^{-1}$)	B_s (10^{12} G)	B_{LC} (10^5 G)	PD (%)	References
B0531+21	1.24	0.033	4.22	4.6	3.78	9.80	5.2 ± 0.3	(1)
							5.5 ± 0.1	(2)
B0540–69	1.67	0.050	4.79	1.5	4.98	3.62	5.0 ± 2.0	(3)
							16.0 ± 4.0	(4)
							≈ 5.0	(5)
							10.4	(5)
B1509–58	1.56	0.151	15.3	0.17	15.40	0.42	10.4	(5)
B0833–45	11.3	0.089	1.25	0.069	3.38	0.44	8.1 ± 0.7	(6)
							9.4 ± 4	(7)
							8.5 ± 0.8	(5)
B0656+14	111	0.384	0.55	0.00038	4.66	0.007	11.9 ± 5.5	this work

Notes. For the Crab, a value of the polarisation was obtained from phase-resolved observations by Słowiowska et al. (2009, 2012).

References. (1) Moran et al. (2013); (2) Słowiowska et al. (2012); (3) Lundqvist et al. (2011); (4) Mignani et al. (2010); (5) Wagner & Seifert (2000); (6) Moran et al. (2014); (7) Mignani et al. (2007).

that the phase-average value obtained from their data would be very low and, possibly, close to our value.

We also obtained a first measurement of the PA of the phase-averaged optical polarisation of PSR B0656+14. The value ($125.8^\circ \pm 13.2^\circ$) is close to the PA of the pulsar proper motion ($93.12^\circ \pm 0.38^\circ$; Brisken et al. 2003). Since the difference between the two angles is within 3σ , an alignment between the two vectors is possible, as clearly seen in the Crab pulsar (Moran et al. 2013) and, approximately, in the Vela pulsar also (Moran et al. 2014). Evidence of alignment between the polarisation and proper motion vectors is also found at radio wavelengths (Johnston et al. 2005; Noutsos et al. 2012). For PSR B0656+14, radio polarisation measurements at 3.1 GHz give a PA of $-86^\circ \pm 2^\circ$ (Johnston et al. 2007) at the phase of closest approach of the magnetic pole to the observer’s line of sight. This value is very close (mod 180°) to the proper motion PA and, accounting for the phase-dependent variations of the radio polarisation PA and the measurement uncertainties, compares to our phase-averaged optical polarisation PA. Assuming that the pulsar proper motion vector is always aligned with the spin axis (e.g. Lai et al. 2001; Johnston et al. 2005, 2007; Noutsos et al. 2012), the alignment with the optical polarisation direction might be explained by a similar optical emission geometry and inclination angle α of the magnetic axis with respect to the spin axis for the Crab and Vela pulsars and PSR B0656+14. This is suggested by their two-peak optical light curves and possibly similar values of α (e.g. Johnston et al. 2005; McDonald et al. 2011; Zhang & Jiang 2006). For both the Crab and Vela pulsars, the phase-averaged optical polarisation and proper motion vectors are also approximately aligned with the axis of symmetry of their X-ray PWNe, which are thought to coincide with the pulsar spin axis. Unfortunately, for PSR B0656+14 only a tentative evidence of an X-ray PWN has been found so far (Pavlov et al. 2002).

With our VLT measurement, linear polarisation values have now been obtained for all the five brightest pulsars identified in the optical (Mignani 2011). Table 1 summarises all the measurements obtained from phase-averaged imaging polarimetry. From a general standpoint, these data suggest that the pulsar phase-averaged polarisation is lower in the optical than in radio (e.g. Weltevrede & Johnston 2008). This might be ascribed to

the difference between incoherent and coherent radiation emission mechanisms in the optical and in radio, respectively. This comparison, however, must be taken with due care since the radio band is much broader than the optical band and the radio PD is frequency dependent. In particular, the radio PD decreases from the MHz to the GHz frequency ranges, probably due to depolarisation effects produced by scattering of the radio waves in the ISM (e.g. Noutsos et al. 2009). X and γ -ray polarisation measurements could confirm that the polarisation level depends on the underlying emission mechanisms. We investigated possible correlations between the phase-averaged optical PD and the pulsar characteristic age τ , the spin period P_s and its derivative \dot{P}_s , the spin-down power \dot{E} , and the pulsar magnetic field measured both at the surface (B_s) and at the light cylinder (B_{LC}). For both the Crab and Vela pulsars, we assumed the recent HST measurements (Moran et al. 2013, 2014) as a reference. We did not include the VLT polarisation measurements of PSR B0540–69 and PSR B1509–58 (Wagner & Seifert 2000), which have no associated errors. The linear fit shows some evidence of a possible increase of PD with τ (Fig. 2a; reduced $\chi_r^2 = 0.38$). Possible trends for an increase of PD with P_s (Fig. 2b; $\chi_r^2 = 0.84$) and for a decrease of PD with \dot{P}_s (Fig. 2c; $\chi_r^2 = 0.33$) are also found. The data also suggest a possible decrease of PD with \dot{E} (Fig. 2d; $\chi_r^2 = 0.58$). Incidentally, the opposite trend is observed in radio, as found, e.g. by observations at 4.9 GHz (von Hoensbroech et al. 1998) and 1.5 GHz (Weltevrede & Johnston 2008), although this sort of trend is more clear at high radio frequencies. Since the optical luminosity scales with \dot{E} (e.g. Mignani et al. 2012), the trend in Fig. 2d would also imply that the fainter pulsars are more strongly polarised than the brighter ones. On the other hand, there is no correlation between the optical PD and B_s (Fig. 2e; $\chi_r^2 = 14.5$), whereas a possible trend for a decrease of PD with B_{LC} is more apparent (Fig. 2f; $\chi_r^2 = 0.65$). To summarise, if our measurement of the PSR B0656+14 polarisation were confirmed the general picture that would emerge would be that the PD tends to be higher in older and less energetic pulsars, and with the lower value of the magnetic field at the light cylinder. The relatively lower values of PD for younger and more energetic pulsars might be due to the optical emission coming from spatially extended regions of the magnetosphere (and possibly

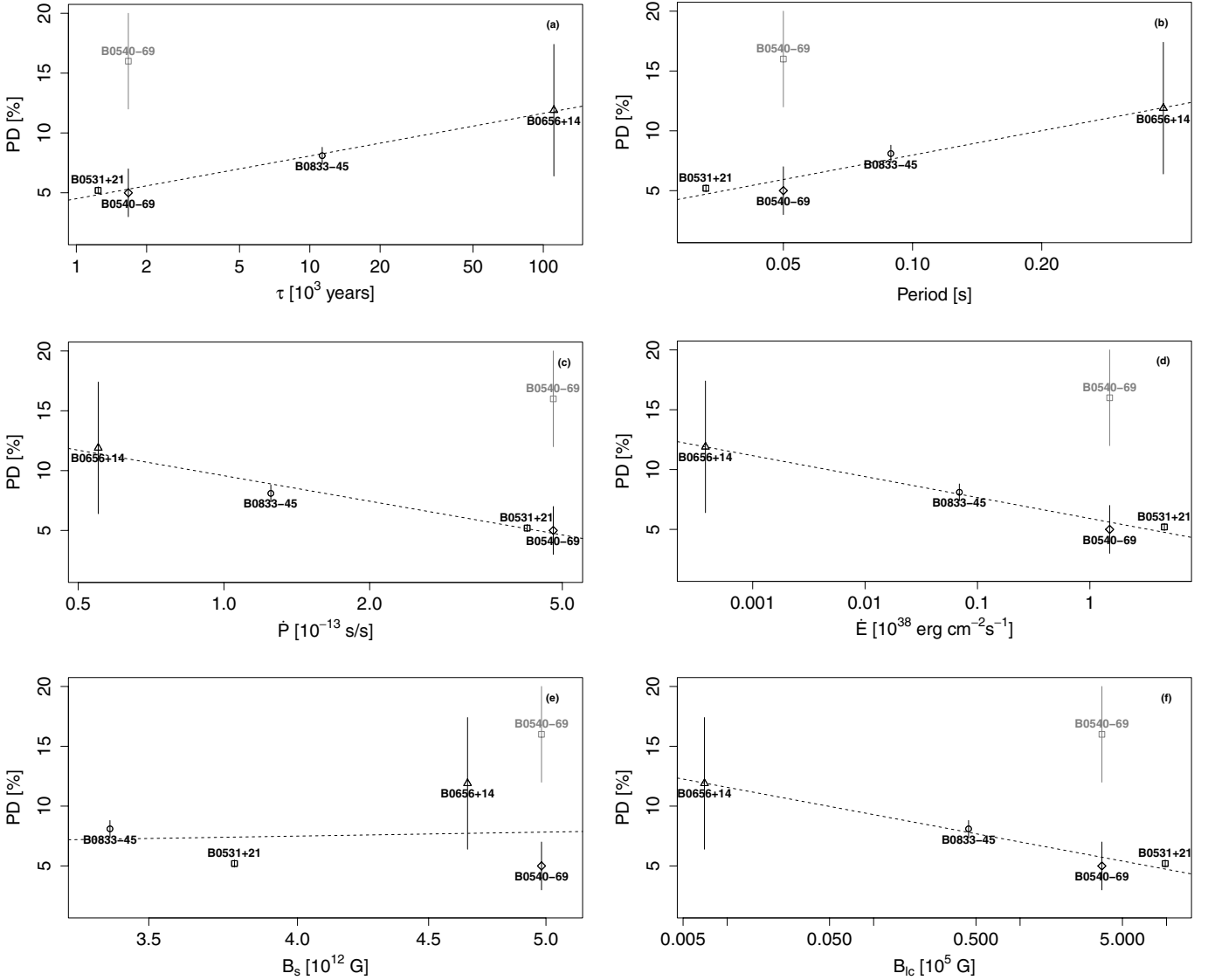


Fig. 2. Polarisation degree as a function of **a)** the pulsar characteristic age τ ; **b)** spin period P_s ; **c)** spin period derivative \dot{P}_s ; **d)** spin-down power \dot{E} ; **e)** magnetic field at the surface B_s ; and **f)** at the light cylinder B_{LC} . The dotted lines show the best fit to the points with a linear function. The point in light grey deviates more than 1σ from the best fit.

forming caustic-like structures). In this case, the resulting intrinsic PD would be lower as a result of effective depolarisation of the radiation from different emitting regions. The emitting regions (related to outer gaps or slot gaps) might shrink in radial extension as the pulsar ages and becomes less energetic. More optical polarisation measurements, covering larger ranges in the parameter space, together with the confirmation of the uncertain measurements, will assess the reality of the observed trends and link them to the pulsar physical properties.

Acknowledgements. This work is dedicated to the memory of our dear friend and colleague, Prof. Janusz Gil. We are indebted to S. Bagnulo and A. Stinton for their help in the observations planning and data analysis. R.P.M. thanks the European Commission Seventh Framework Programme (FP7/2007-2013) for their support under grant agreement No. 267251. P.M. is grateful for his funding from the Irish Research Council (IRC). B.R. acknowledges support by the National Science Centre grant Dec-2011/02/A/ST9/00256. A.S. and K.K. acknowledge the Polish National Science Centre grant Dec-2011/03/D/ST9/00656. We thank the referee for his/her constructive review of our manuscript.

References

- Appenzeller, I., Fricke, K., Fürtig, W., et al. 1998, *The Messenger*, **94**, 1
 Brisken, W.F., Thorsett, S. E., Golden, A., & Goss, W. M., 2003, *ApJ*, **593**, 89
 Boffin, H. M. J. 2014, *The FORS2 User Manual*
 Fossati, L., Bagnulo, S., Mason, E., & Landi Degl’Innocenti, E., 2007, in *The Future of Photometric, Spectroscopic, and Polarimetric Standardization*, *ASP Conf. Ser.*, **364**, 503
 Johnston, S., Hobbs, G., Vigeland, S., et al. 2005, *MNRAS*, **364**, 1397
 Johnston, S., Kramer, M., Karastergiou, A., et al. 2007, *MNRAS*, **381**, 1625
 Hester, J. J. 2008, *ARA&A*, **46**, 127
 Kargaltsev, O., & Pavlov, G. G. 2007, *Ap&SS*, **308**, 287
 Kern, B., Martin, C., Mazin, B., & Halpern, J. P. 2003, *ApJ*, **597**, 1049
 Lai, D., Chernoff, D. F., & Cordes, J. M. 2001, *ApJ*, **549**, 1111
 Lasker, B. M., Lattanzi, M. G., McLean, B. J., et al. 2008, *AJ*, **136**, 735
 Lundqvist, N., Lundqvist, P., Björnsson, C.-I., et al. 2011, *MNRAS*, **413**, 611
 McDonald, J., O’Connor, P., de Burca, D., Golden, A., & Shearer, A. 2011, *MNRAS*, **417**, 730
 Mignani, R. P. 2011, *Adv. Space. Sci.*, **47**, 1281
 Mignani, R. P., Bagnulo, S., Dyks, J., Lo Curto, G., & Słowikowska, A. 2007, *A&A*, **467**, 1156
 Mignani, R. P., Sartori, A., de Luca, A., et al. 2010, *A&A*, **515**, A110
 Mignani, R. P., De Luca, A., Hummel, W., et al. 2012, *A&A*, **544**, A100
 Moran, P., Shearer, A., Mignani, R. P., et al. 2013, *MNRAS*, **433**, 2564

- Moran, P., Mignani, R. P., & Shearer, A. 2014, *MNRAS*, **445**, 835
- Noutsos, A., Karastergiou, A., Kramer, M., Johnston, S., & Stappers, B. W. 2009, *MNRAS*, **396**, 1559
- Noutsos, A., Kramer, M., Carr, P., & Johnston, S. 2012, *MNRAS*, **423**, 2736
- Pavlov, G. G., Zavlin, V. E., & Sanwal, D. 2002, in Neutron Stars, Pulsars, and Supernova Remnants, *MPE Report*, **278**, 273
- Shearer, A., Redfern, R. M., Gorman, G., et al. 1997, *ApJ*, **487**, L181
- Słowikowska, A., Kanbach, G., Kramer, M., & Stefanescu, A. 2009, *MNRAS*, **397**, 103
- Słowikowska, A., Mignani, R.P., Kanbach, G., & Krzeszowski, K. 2013, in Electromagnetic Radiation from Pulsars and Magnetars, *ASP Conf. Ser.*, **466**, 37
- Stetson, P. B. 1994, *PASP*, **106**, 250
- Verbiest, J. P. W., Weisberg, J. M., Chael, A. A., Lee, K. J., & Lorimer, D. R. 2012, *ApJ*, **755**, 39
- von Hoensbroech, A., Kijak, J., & Krawczyk, A. 1998, *A&A*, **334**, 571
- Wagner, S. J., & Seifert, W. 2000, in Pulsar Astronomy – 2000 and Beyond, *ASP Conf. Ser.*, **202**, 315
- Weltevrede, P., & Johnston, S. 2008, *MNRAS*, **391**, 1210
- Wiktorowicz, S., Ramirez-Ruiz, E., Illing, R. M. E., & Nofi, L. 2015, AAS Meeting, 225, 421.01
- Zhang, L., & Jiang, Z. J. 2006, *A&A*, **454**, 537
- Zharikov, S., Mennickent, R. E., Shibanov, Yu., & Komarova, V. 2007, *Ap&SS*, **308**, 545